

A new structure of $\text{Nd}_{1+\varepsilon}\text{Fe}_4\text{B}_4$ phase in NdFeB magnet

S. C. Wang

Materials Research Group, School of Engineering Science, The University of Southampton SO17 1BJ UK;
and Electron Microscopy Centre, Faculty of Engineering and Science, The University of Southampton, UK
E-mail: wangs@soton.ac.uk

Y. Li

School of Metallurgy and Materials, The University of Birmingham, B15 2TT, UK

Sintered NdFeB magnets are relatively complex multiphase systems containing $\text{Nd}_2\text{Fe}_{14}\text{B}$ matrix and about 15% of other intermetallics such as $\text{Nd}_{1+\varepsilon}\text{Fe}_4\text{B}_4$, Nd-oxides (Nd-rich phase), etc. Boron rich $\text{Nd}_{1+\varepsilon}\text{Fe}_4\text{B}_4$ forms in irregularly distributed heavily faulted grains of roughly the same size as those of the $\text{Nd}_2\text{Fe}_{14}\text{B}$ phase [1]. The Curie temperature of this phase is 13K and, therefore, it is not ferromagnetic at room temperature and is deleterious to the magnetic properties of the magnets.

$\text{Nd}_{1+\varepsilon}\text{Fe}_4\text{B}_4$ (where $\varepsilon \approx 0.1$) have been constructed by two different repeat units of Nd and Fe-B substructures along the c -axis with the identical a [2,3]. The Nd substructure has a body-centred tetragonal (bct) structure with $I4/mmm$ space group, and the Fe-B sub-structure has a primitive tetragonal structure with $P4_2/nm$ space group [2,4]. The corresponding atomic coordinates for two substructures are shown in Table 1. The combination of two substructures with slightly different $c_{\text{Fe-B}}$ and c_{Nd} parameters will form different commensurate structure for $\text{Nd}_{1+\varepsilon}\text{Fe}_4\text{B}_4$. Up to now, three kinds of structures have been reported as shown in Table 2. The c parameter for $\text{Nd}_{1+\varepsilon}\text{Fe}_4\text{B}_4$ can be deduced from $c = m \cdot c_{\text{Fe-B}} = n \cdot c_{\text{Nd}}$, where m and n are integers. And the corresponding composition coefficient $\varepsilon = n / m - 1$. In this study, we will report a new commensurate structure which contains seven units of Fe-B sub-structure and eight units of Nd sub-structure.

Table 1 The substructures reported unit cell parameters for $\text{Nd}_{1+\varepsilon}\text{Fe}_4\text{B}_4$

Space group	Atom	Site	Coordinate		
$I4/mmm$	Nd	$2a$	0	0	0
$P4_2/nm$	Fe	$8i$	0.127	0.127	0.1349
	B	$8i$	0.068	0.068	0.639

Table 2 The reported unit cell parameters for $\text{Nd}_{1+\varepsilon}\text{Fe}_4\text{B}_4$

Lattice parameters of $\text{Nd}_{1+\varepsilon}\text{Fe}_4\text{B}_4$		c parameters of substructures			Composition of sintered alloy (at. %)	Reference
a (nm)	c (nm)	$c_{\text{Fe-B}}$ (nm)	c_{Nd} (nm)	n/m		
0.7133	14.457	0.3899	0.3519	41/37	$\text{Nd}_{12}\text{Fe}_{44}\text{B}_{44}$	[2]
0.7117	3.507	0.3897	0.3502	10/9	$\text{Nd}_{12.5}\text{Fe}_{43.8}\text{B}_{43.8}$	[3]
0.71	6.631	0.39	0.349	19/17	$\text{Nd}_{14}\text{Fe}_{44}\text{B}_{42}$	[5]

The NdFeB magnets used for this study were supplied by Philips Component Ltd. and had nominal composition $\text{Nd}_{15}\text{Fe}_{76.5}\text{B}_7(\text{Dy,Nb,Al})_{1.5}$ (at. %) [6]. The magnets were produced by a powder metallurgy method (ingot \rightarrow HD \rightarrow jet milling \rightarrow powder alignment \rightarrow pressing \rightarrow sintering) and were finally demagnetised. TEM foils were prepared using ion milling (see [7] for detail). TEM observations were carried out in a JEOL 4000FX.

Fig. 1 shows a TEM bright field micrograph of $\text{Nd}_{1+\varepsilon}\text{Fe}_4\text{B}_4$ phase surrounded by $\text{Nd}_2\text{Fe}_{14}\text{B}$ matrix in the as-received sample. Figs. 2(a,b) show two selected area electron diffraction (SAD) patterns from $\text{Nd}_{1+\varepsilon}\text{Fe}_4\text{B}_4$ phase. To determine the n/m value, two substructures of Nd and Fe-B with the relationship of $[100]_{\text{Nd}} // [100]_{\text{Fe-B}}$ & $[001]_{\text{Nd}} // [001]_{\text{Fe-B}}$, have been used to simulate the patterns. It is found that the commensurate

structure with $n/m = 8/7$, as shown in Fig. 3 (double diffractions are not considered), can elucidate the basic patterns of Fig. 2. Such a structure has not been given so far in this compound family, but the same n/m value was reported in $\text{Gd}_{1+\epsilon}\text{Fe}_4\text{B}_4$ [8] with the space group of Pccn. Based on the atomic coordinates of $\text{Gd}_{1+\epsilon}\text{Fe}_4\text{B}_4$, [001] and [010] zones have been simulated as shown in Figs. 4(a, b) (using Diffract 1.2 software, Birmingham University). Comparing to the correspondences of Figs. 2(a,b), the simulated diagrams explain very well the real diffraction patterns, in both intensities and spacings of diffractions. The lattice parameters for $\text{Nd}_{1+\epsilon}\text{Fe}_4\text{B}_4$ are $a = 0.71 \pm 0.005$ nm, $c = 2.74 \pm 0.05$ nm, and the composition of the phase is deduced to be $\text{Nd}_2\text{Fe}_7\text{B}_7$ ($\epsilon = 0.143$).

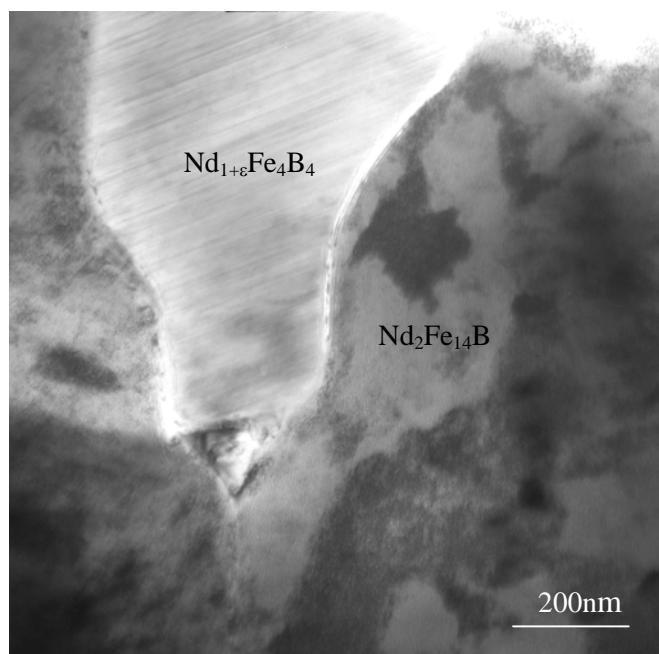


Fig. 1 Bright field image of the $\text{Nd}_{1+\epsilon}\text{Fe}_4\text{B}_4$ phase in the as-received sample.

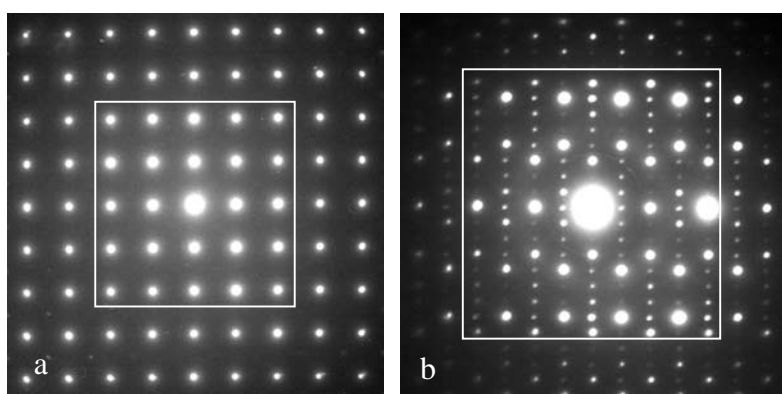


Fig. 2(a,b) Selected area electron diffraction patterns from $\text{Nd}_{1+\epsilon}\text{Fe}_4\text{B}_4$ phase.

The reason for the existence of such a structure is unknown. However, we notice that the higher ratio of $n_{\text{Nd}}/m_{\text{Fe-B}}$ (column 5 of Table 2) corresponds to the higher ratio of Nd/Fe in as cast alloys (column 6 of Table 2). Accordingly, it is argued that the formation of the new structure is related to the alloy composition.

In conclusion, a new structure for $\text{Nd}_{1+\epsilon}\text{Fe}_4\text{B}_4$ phase has been observed, which has the same structure as $\text{Gd}_{1+\epsilon}\text{Fe}_4\text{B}_4$. The compound has Pccn structure with $a = 0.71$ nm and $c = 2.74$ nm, and its composition was found to be $\text{Nd}_2\text{Fe}_7\text{B}_7$.

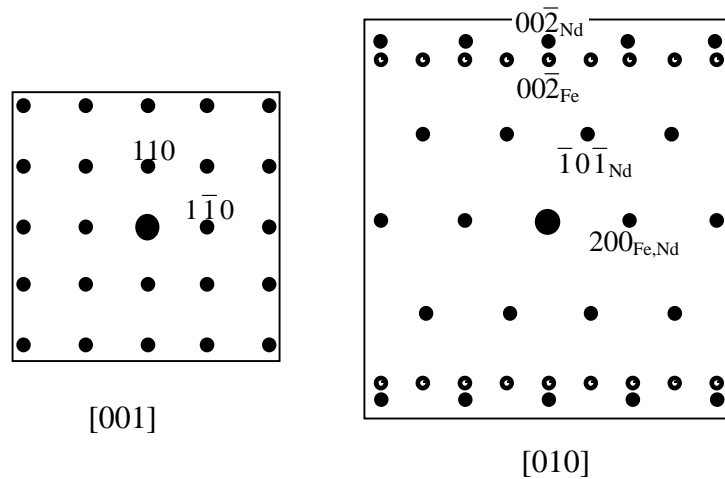


Fig. 3 The indexed diagrams of two sub-structures of Nd and Fe-B with the relationship of $[100]_{\text{Nd}} // [100]_{\text{Fe-B}}$ & $[001]_{\text{Nd}} // [001]_{\text{Fe-B}}$. The solid and shadowed circles represent Nd sub-structure ($I4/mmm$, $a = 0.71$ nm, $c = 0.343$ nm) and Fe-B sub-structure ($P4_2/ncm$, $a = 0.71$ nm, $c = 0.392$ nm), respectively. The double diffractions are not considered.

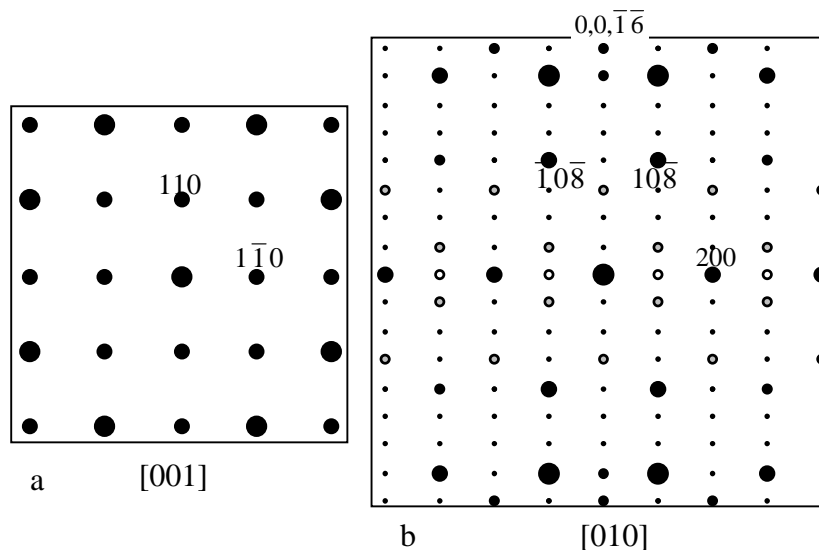


Fig. 4(a-b) The indexed diagrams for $[001]$ & $[010]$ zones of $\text{Nd}_{1+\epsilon}\text{Fe}_4\text{B}_4$ based on $Pccn$ ($\epsilon \sim 0.143$) with lattice parameters $a = 0.71$ nm, $c = 2.74$ nm. The solid and open circles represent the actual and double diffractions, and the shadowed circles are attributed by both.

Acknowledgment

One of the authors (YL) would like to thank professors I.R. Harris, I.P. Jones of Birmingham University, UK and Professor M. Aindow of University of Connecticut, USA for the PhD supervisions. Financial support was provided by the committee of Vice Chancellors and Principals under the Oversea Research Scholar (ORS) Scheme, School of Metallurgy and Materials, The University of Birmingham and School of Engineering Science, The University of Southampton.

References

1. X. J. Yin, I. P. Jones and I. R. Harris, *J. Magn. Magn. Mat.* **125** (1993) 91.
2. A. Bezing, H. F. Braun, J. Muller and K. Yvon, *Solid State Commun.* **55** (1985) 131.
3. D. Givord, J. M. Moreau and P. Tenaud, *Solid State Commun.* **55** (1985) 303.
- 4 D. Givord, P. Tenaud and J. M. Moreau, *J. Less-common Met.* **115** (1986) L7.
5. A. Bezing, K. Yvon, H. F. Braun, J. Muller and H. U. Nissen, *Phys. Rev. B* **36** (1987) 1406.
6. Y. Li, H. E. Evans, I. R. Harris and I. P. Jones, *Oxidation of Metals*. **59** (2003) 167.
- 7 S. C. Wang and Y. Li, *J. Magn. Magn. Mater.* 2005 in press.
8. D. Givord and P. Tenaud, *J. Less-common Met.* **123** (1986) 109.